We are IntechOpen, the world's leading publisher of Open Access books Built by scientists, for scientists

4,800
Open access books available

122,000
International authors and editors

135M
Downloads

Our authors are among the

154
Countries delivered to

TOP 1%
most cited scientists

12.2%
Contributors from top 500 universities

WEB OF SCIENCE™

Selection of our books indexed in the Book Citation Index in Web of Science™ Core Collection (BKCI)

Interested in publishing with us?
Contact book.department@intechopen.com

Numbers displayed above are based on latest data collected.
For more information visit www.intechopen.com

6

Image Representation Using Fuzzy Morphological Wavelet

Chin-Pan Huang
Department of computer and communication engineering,
Ming Chuan University
Taiwan, ROC

1. Introduction

Multiresolution techniques for image processing have grown very rapidly in the last few years (Burt & Adelson, 1983, Heijmans & Goutsias, 2000, Goutsias & Heijmans, 2000). The bank-of-filters implementation method, based on the discrete wavelet transform (Heijmans & Goutsias, 2000, Mallat, 1989), has been very significant. However, in general, such an implementation has limitations due to intensive computation, sequential implementation and lack of the geometrical information in the processing. Moreover, the theoretical extension from one-dimension to two-dimension is complex (Vaidyanathan, 1993). In this paper, we propose a technique based on fuzzy mathematical morphology (Sinha & Dougherty, 1992) to implement the multiresolution analysis, which is analogous to discrete wavelet transformation, in one- and two-dimensions. Fuzzy morphological operators, similar to conventional morphological operators (Sternberg, 1983, Haralick et al., 1987), are non-linear well suited for efficient implementation using parallel computing. Moreover, they have the ability to extract geometrical information in signals by appropriate transformations. Furthermore, our method can be easily extended to two-dimension.

Rcently, Mallat et al. (Heijmans & Goutsias, 2000, Mallat, 1989) have developed a hierarchical structure to decompose and reconstruct a signal based on one-dimensional wavelet orthogonal bases. Haralick et al. (Haralick et al., 1989) and Heijmans (Heijmans & Toet, 1991) have developed a morphological sampling theory that gives a theoretical basis to reconstruct sampled signals. Its application is constrained by sampling conditions. Toet (Heijmans & Toet, 1991) has proposed morphological approach using many scales but identical shape as structuring function. This approach has some computational benefits due to using the morphological filter instead of the linear filter. Although this method takes care of the geometrical information of the processing signal it uses only a single identical shape of structure in each scale. This decomposition structure is actually same as Burt and Adelsons' (Burt & Adelson, 1983) work which has the problem of 4/3 redundant for a sample representation (Kronander). Cha (Cha & Chaparro, 1999) has proposed a morphological wavelet transform which uses conventional morphology and is suitable for positive signals. Our objective is to develop a representation taking the advantage of the methods reviewed above while overcome some problems they have.

Source: Pattern Recognition Techniques, Technology and Applications, Book edited by: Peng-Yeng Yin,
ISBN 978-953-7619-24-4, pp. 626, November 2008, I-Tech, Vienna, Austria

In new paper, we propose a fuzzy morphological approach to represent one- and two-dimensional signals, that extends the geometrical decomposition (Pitas & Venetsanopoulos, 1990, Pitas, 1991, Pitas & Venetsanopoulos, 1991) of signals using multiple structuring functions (Song & Delp, 1990) into the fuzzy morphological frame. We will develop a fuzzy morphological interpolator (FMI) which along with a hierarchical pyramid-like structure yields a multiresolution signal representation called fuzzy morphological wavelet (FMW). Our algorithm is illustrated by means of experiment to one- and two-dimensional signals for signal and image analysis and shape recognition.
In section 2, we briefly review fuzzy mathematical morphology. In section 3, we develop the one-dimensional FMW representation. A one-dimensional FMI algorithm is formulated first. We consider then fast pyramid implementation for the first and second order interpolators. In section 4, we extend our algorithm to two-dimensions. We discuss a two dimensional FMI. We then develop a two-dimensional FMW representation based on one-dimensional FMI and the two-dimensional FMI. A fast two-dimensional pyramid implementation is also derived. In section 5, we apply our representation to data compression and shape recognition, demonstrating the advantage of our representation over the commonly used Daubechies' wavelet and Fourier descriptor methods. Finally, concluding remarks are given in section 6.

2. Fuzzy mathematical morphology

Recently, Sinha and Dougherty (Sinha & Dougherty, 1992) proposed to consider fuzzy set theory (Zadeh, 1965) instead of the classical set theory to develop mathematical morphology. They have in fact, obtained a new approach that considers simultaneously binary and multilevel morphology. The concept of "umbra" is not longer needed to develop the multilevel case. Morphological operations are then developed on the "fuzzy" fitting so that for crisp sets the fitting still remains characterized as either 0 or 1, but fuzzy or no-crisp sets it is possible to have a fitting characterized by a value between 0 and 1. The closer to unity, the better the fitting of the structuring element. As in the classical morphology, fuzzy morphology (Sinha & Dougherty, 1992) also consists in transforming a fuzzy set into another. Such a transformation is performed by means of a fuzzy structuring set containing the desired geometric structure.
If we let X be the universe of discourse and x be its generic element, the difference between crisp and fuzzy sets is the characteristic function of a crisp set C is defined as $\mu C:X \to \{0,1\}$ while the membership function $\mu F:X \to [0,1]$ of a fuzzy set F is defined so that $\mu F(x)$ denotes the degree to which x *belongs* to the set F. Among the different operations on fuzzy sets (Dubois & Prade, 1980), the following are important that operations will be used later:

a. Complement operation:

$$\mu F^c(x) = 1 - \mu F(x)$$

b. Translation of a fuzzy set F by a vector $v \in X$:

$$\mu T(F;v)(x) = \mu F(x - v)$$

c. Reflection of a set F:

$$\mu - F(x) = \mu F(-x)$$

d. Bold union of two sets F and G :

$$\mu F \Delta G(x) = min\left[1, \mu F(x) + \mu G(x)\right] \tag{1}$$

e. Bold intersection $F \nabla G$:

$$\mu F \nabla G(x) = max\left[0, \mu F(x) + \mu G(x) - 1\right] \tag{2}$$

The degree of fitting of a set A into a set B is measured by an inclusion grade operator

$$\begin{aligned} I(A,B) &= \inf_{x \in X} \mu A^c \Delta B(x) \\ &= 1 + min\left\{0, \inf_{x \in X}\left[\mu B(x) - \mu A(x)\right]\right\} \end{aligned} \tag{3}$$

where Δ is the bold union operator. According to the above index the degree of subsethood of two crisp sets A, B is either 0 or1, while for fuzzy sets C and D $I(C,D) \in \left[0,1\right]$. Moreover, if $C \subseteq D$ then $I(C,D) = 1$ and in general $0 \le I(C,D) \le 1$. Using such an index (Sinha & Dougherty, 1992) has shown the erosion operation can be defined, and from it the dilation, opening and closing operators are obtained. In fact, if $f(n)$ is a multilevel and $k(n)$ is a structuring element with supports F and K and membership function $\mu f(n)$ and $\mu k(n)$ then we have

Erosion:

$$\begin{aligned} \mu f \Theta k(n) &= I(T(k;n), f) \\ &= \min_{i \in K}\left\{min\left[1, 1 - \mu k(i) + \mu f(n+i)\right]\right\} \end{aligned} \tag{4}$$

Dilation:

$$\begin{aligned} \mu f \oplus k(n) &= \mu(f^c \Theta - k)^c(n) \\ &= \max_{i \in K}\left\{max\left[0, \mu k(i) + \mu f(n-i) - 1\right]\right\} \end{aligned} \tag{5}$$

Opening: $$\mu f \circ k(n) = \mu(f \Theta k) \oplus k(n)$$

Closing: $$\mu f \bullet k(n) = \mu(f \oplus k) \Theta k(n)$$

3. Fuzzy Morphological Wavelet (FMW) representation

This representation is analogous to the multiresolution decomposition (Heijmans & Goutsias, 2000, Mallat, 1989) and the morphological wavelet transform (Cha & Chaparro, 1999). We first introduce a fuzzy morphological interpolation (FMI) and then develop the FMW representation

3.1 Fuzzy morphological interpolation

In (Haralick et al., 1989, Heijmans & Toet, 1991), it is shown that under special conditions a morphological sampling theorem permits the reconstruction of sampled signals. We show in this section, that under general conditions one can develop an interpolation algorithm to

reconstruct sampled membership functions by adapting the fuzzy structuring functions. Furthermore, fast computation algorithms can be obtained.

Let $F = \{n \mid 0 \le n \le M-1\}$ be the domain of the given signal $f(n)$ and its membership function $\mu f(n)$, and let $K = \{n \mid 0 \le n \le N-1\}$ be the domain of the fuzzy structuring function $\mu k_i(n)$ and the window function $W(n)$. Assuming $M >> N$ and $K \subset F$ we then let $S = \{m \mid m = nQ, 0 \le n \le (N-1)/Q\}$ be the sampling domain where Q is the sampling rate. Choosing the sampling rate Q and the window length N appropriately, $Q < N$, we then define the positive integer $\theta = (N-1)/Q$ as the order of the interpolator.

Assuming there is no a-priori information about the geometrical structure of the membership function, a set of fuzzy structuring functions based on ordered normalized orthogonal polynomials (e.g., the NDLO (Neuman & Schonbach, 1974)) can be used for the interpolation.

For a windowed membership function $\mu z(n),\ n \in K$, the sampled membership function in a window is defined as

$$\mu z\downarrow_s (n) = \begin{cases} \mu z(n) & n \in K \cap S \\ undefined & n \in K \cap \overline{S} \end{cases} \tag{6}$$

Thus, $\mu z\downarrow_s (n)$ is equal to $\mu z(n)$ every Q sample but is undefined at other samples in the window. The sampled membership function with 0 for $n \in K \cap \overline{S}$, denoted as $\mu z\downarrow_s^0 (n), n \in K$ is defined as

$$\mu z\downarrow_s (n) = \begin{cases} \mu z(n) & n \in K \cap S \\ 0 & n \in K \cap \overline{S} \end{cases} \tag{7}$$

The function $\mu z\downarrow_s^0 (n)$ is equal to $\mu z(n)$ every Q sample but is 0 at other samples in the window.

Just as in (Haralick et al., 1989) we can obtain a minimum approximation (fitting from below), denoted as $\mu^v f_{min}(n)$, and a maximum approximation (fitting from above), denoted as $\mu^v f_{max}(n)$, in a window $[0, N-1]$ by considering the approximation of the signal membership function $\mu^v z_0(n), n \in K$.

3.2 General interpolation algorithm

The following algorithm provides a way to interpolate the given samples of a signal membership function in a window. It basically obtains an adaptive approximation of the windowed membership function in a recursive way. This geometric decomposition permit us, just as in the fuzzy morphological polynomial representation(Huang & Chaparro, 1995), to obtain the adaptation coefficients as well as minimum and maximum reconstructions of the membership function. Our fuzzy morphological interpolation algorithm in a window v is as follows:

1. Frame definition:

$$\mu^v x_0\downarrow_s (n) = \mu f\downarrow_s (n) \times W(n - vN)$$

2. Membership function selection (min and/or max approximation)

$$\mu^{\nu} z_0 \downarrow_s (n) = \mu^{\nu} x_0 \downarrow_s (n) \text{ and/or } \mu^{\nu} z_0 \downarrow_s (n) = \mu^{\nu} x_0^c \downarrow_s (n) = 1 - \mu^{\nu} x_0 \downarrow_s (n).$$

3. Adaptation:

$$\begin{aligned} \mu^{\nu} z_i \downarrow_s \circ a_i k_i \downarrow_s (n) &= a_i \mu k_i \downarrow_s (n) \\ \mu^{\nu} \widetilde{f}_i (n) &= a_i \mu k_i (n) \end{aligned} \tag{8}$$

4. Residual calculation:

$$\mu^{\nu} z_{i+1} \downarrow_s (n) = \mu^{\nu} z_i \downarrow_s (n) - \mu^{\nu} \widetilde{f}_i \downarrow_s (n) \tag{9}$$

5. Termination criterion: For frame ν if $i = \theta$ stop and consider next frame; otherwise increment i and go to step 3. If all frames are done then stop. Consider both the minimum (i.e., when $\mu^{\nu} z_0 \downarrow_s (n) = \mu^{\nu} x_0 \downarrow_s (n)$) and the maximum (i.e., when $\mu^{\nu} z_0 \downarrow_s (n) = 1 - \mu^{\nu} x_0 \downarrow_s (n)$) interpolations.

In the above, $\circ$ stands for fuzzy morphological opening, and $\mu\, y_i \downarrow_s$ is a sampled membership function. The minimum and maximum reconstruction interpolated membership functions in a frame, are found to be equal

$$\mu^{\nu} f_{min}(n) = \sum_{i=0}^{\theta} \mu^{\nu} \widetilde{f}_i (n) = \sum_{i=0}^{\theta} a_i \mu k_i (n) \tag{10}$$

$$\mu^{\nu} f_{max}^c (n) = \sum_{i=0}^{\theta} \mu^{\nu} \widetilde{f}_i (n) = \sum_{i=0}^{\theta} a_i \mu k_i (n) \tag{11}$$

$$\mu^{\nu} f_{max}(n) = 1 - \mu^{\nu} f_{max}^c (n) \tag{12}$$

Whether to choose a minimum or a maximum reconstruction in the ν^{th} frame is determined by comparing the corresponding error. The error of the minimum interpolations at the given sampled pixel is defined as

$$\mu^{\nu} e_{min}(n) = \left| \mu^{\nu} x_0 \downarrow_s^0 (n) - \mu^{\nu} f_{min} \downarrow_s^0 (n) \right| \tag{13}$$

The error of the maximum interpolations at the given sampled pixel is defined as

$$\mu^{\nu} e_{max}(n) = \left| \mu^{\nu} x_0 \downarrow_s^0 (n) - \mu^{\nu} f_{max} \downarrow_s^0 (n) \right| \tag{14}$$

where $\mu^{\nu} x_0(n)$ is the given membership function, $\mu^{\nu} f_{min}(n)$ and $\mu^{\nu} f_{max}(n)$ are the minimum and maximum interpolation membership functions, respectively. The reconstruction error for the minimum ($\mu^{\nu} e_{tmi}$) and maximum ($\mu^{\nu} e_{tma}$) interpolation in a window is defined as

$$\mu^{\nu} e_{tmi} = \sum_{n=0}^{N-1} \left| \mu^{\nu} x_0(n) - \mu^{\nu} f_{min}(n) \right| \tag{15}$$

$$\mu^{\nu} e_{tma} = \sum_{n=0}^{N-1} \left| \mu^{\nu} x_0(n) - \mu^{\nu} f_{max}(n) \right| \tag{16}$$

where the $\mu^{\nu} x_0(n)$ is the given membership function, $\mu^{\nu} f_{min}(n)$ and $\mu^{\nu} f_{max}(n)$ are the minimum and maximum interpolation membership functions, respectively.

3.3 Properties

The following propositions will give insight on how the FMI works and how to calculate the adaptive coefficients $\{a_i\}$. Here, we work on a frame signal only, and thus the superscript ν can be omitted.

Proposition 1. Given $\mu^{\nu} z_i(n),\ \mu^{\nu} k_i(n)$, $n \in K \cap S,\ a_i \in [0,1]$ then

$$\mu^{\nu} z_i \mid \circ a_i k_i(n) = max\left[0, a_i \mu k_i(n) + \mu_c - 1\right],\ n \in K \cap S \tag{17}$$

where $\mu_c = 1 + min\left\{0, min_{\ell}\left[\mu z_i(\ell) - a_i \mu k_i(\ell)\right]\right\},\ \ell \in K \cap S$

Proposition 2. If $\mu^{\nu} z_i(n),\ \mu^{\nu} k_i(n)$, $n \in K \cap S,$ then there exists an optimum $a_i \in [0,1]$ such that $\mu^{\nu} z_i \mid \circ a_i k_i(n) = a_i \mu k_i(n)$, for $n \in K \cap S,$ if and only if the following *optimum* condition is satisfied

$$\min_{\ell \in K \cap S} \left[\mu z_i(\ell) - a_i \mu k_i(\ell)\right] \mu_c = 0 \tag{18}$$

Proposition 3. If *optimum* condition is met then:

i. $\left\{ a_i = \min_{\substack{\ell \in K \cap S \\ \mu k_i(\ell) \neq 0}} \left\{ \frac{\mu z_i(\ell)}{\mu k_i(\ell)} \right\} \right\}$

ii. $a_0 = \min_{\ell \in K \cap S} \left[\mu z_0(\ell)\right]$

iii. $0 \le a_i \le \min_{\ell \in K \cap S} \mu z_i(\ell) \le 1$

iv. $0 \le \mu z_{i+1}(\ell) \le \mu z_i(\ell) \le 1,\ \ell \in K \cap S$

According to the above properties, a_i can be computed uniquely. When using orthogonal polynomials to generate the structuring functions, we need to consider the shifted and normalized orthogonal polynomials $\mu g_i(n)$ and their complements $\mu g_i^c(n)$. To determine either $\mu g_i(n)$ or $\mu g_i^c(n)$ is to be chosen as $\mu k_i(n)$ in the representation, we calculate the corresponding reconstruction errors using equation (15) or (16) and choose the one that gives the smaller error.

3.4 First and second orderinterpolation

The first-order or linear interpolator ($\theta = 1,\ N = 3,\ Q = 2$) keeps the sampled points and provides interpolated values in between using either the minimum or maximum

interpolation. The second-order or quadratic interpolator ($\theta = 2,\ N = 5,\ Q = 2$) performs similarly with an additional condition on convexity. Convexity is tested by simply checking that the middle sample of the membership function is greater than or equal to the average of the other two points. For both interpolators it is possible to develop a closed form formula for calculating the interpolated points. The following propositions provide theoretical basis for the fast computation algorithms to be discussed later. Proofs are easily obtained by following the above interpolation algorithm.

Proposition 4. For a first order interpolator the windowed sampled membership function is

$$\mu x_0 \downarrow_s (n) = \{\mu f(0), *, \mu f(2)\}.$$

Using either minimum or maximum reconstruction the interpolation results is

$$\mu \overline{f}(n) = \{\mu f(0), 0.5[\mu f(0) + \mu f(2)], \mu f(2)\}.$$

Proposition 5. For a second order interpolator the windowed sampled membership function is

$$\mu x_0 \downarrow_s (n) = \{\mu f(0), *, \mu f(2), *, \mu f(4)\}.$$

Using the minimum interpolation under convexity conditions or the maximum interpolation under concavity condition the interpolation result is

$$\mu \overline{f}(n) = \{\mu f(0), \mu \widetilde{f}(1), \mu f(2), \mu \widetilde{f}(3), \mu f(4)\} \tag{19}$$

where $\mu \widetilde{f}(1) = 0.375\mu f(0) + 0.75\mu f(2) - 0.125\mu f(4)$ and
$\mu \widetilde{f}(3) = -0.125\mu f(0) + 0.75\mu f(2) + 0.375\mu f(4)$.

3.5 Higher order interpolation

When the order is greater than two, we do not have the assurance that the sampled points are kept, which as we will see is very important for the FMW representation. As a solution, we use the following algorithm to select the minimum or maximum interpolation and to correct the sampled points whenever necessary. In the case when the errors $\mu^v e_{min}(n) = 0, \mu^v e_{max}(n) = 0$ (see equations (13) and (14) then the interpolated membership function of the v^{th} frame be

$$\mu^v \overline{f}(n) = \mu^v f_{min}(n) \tag{20}$$

$$\mu^v \overline{f}(n) = \mu^v f_{max}(n) \tag{21}$$

In this case the given sample points are preserved. Otherwise we would have that either be $\mu^v e_{min}(n) \le \mu^v e_{max}(n)$ in which case the interpolated membership function at the v^{th} frame is given by

$$\mu^v \overline{f}(n) = \mu^v x_0 \downarrow_s^0 (n) + \mu^v f_{min} \uparrow_0^s (n) \tag{22}$$

or

$$\mu^{v}\overline{f}(n)=\mu^{v}x_{0}\downarrow_{s}^{0}(n)+\mu^{v}f_{max}\downarrow_{0}^{s}(n) \tag{23}$$

when $\mu^{v}e_{min}(n)>\mu^{v}e_{max}(n)$ and where $\mu^{v}x\downarrow_{0}^{s}(n)$ is defined as

$$\mu^{v}x\downarrow_{0}^{s}(n)=\mu^{v}x(n)-\mu^{v}x\downarrow_{s}^{0}(n)=\begin{cases}0 & n\in K\cap S\\ \mu^{v}x(n) & n\in K\cap\overline{S}\end{cases}$$

where the set $\overline{S}$ is a complement of set S. This will guarantee that the given samples remain unchanged and the other values are interpolated. Knowing which of these situations occurred will allow us to proceed accordingly in the synthesis. In the case third or higher order interpolation both minimum and maximum interpolation need to be done simultaneously and the comparing the errors $\mu^{v}e_{min}(n)$ and $\mu^{v}e_{max}(n)$ and decide which of (20) to (23) to use. This algorithm guarantees perfect reconstruction.

4. Fuzzy morphological wavelet implementation

The wavelet representation (Heijmans & Goutsias, 2000, Mallat, 1989) has received a great deal of attention in image processing. Its implementation is done with a bank of filters. In this section, we show a realization of the basic idea behind the wavelet representation using the FMI algorithm presented before. Our implementation involves no phase in the output and allows perfect reconstruction. We first present the FMW representation using the first and second order interpolation and then present the representation using higher order interpolators.

Let $f_0(n)=f(n)$ be the input signal and $f_i(n)$ be the i^{th} level signal. Let $d_i(n)$ be the i^{th} error signal corresponding to the difference between the i^{th} level signal and its fuzzy morphological interpolated signal. Let **L** be the linear fuzzifier and **D** be the linear defuzzifier described before. Let **H** be the interpolator described in the last section. Let $\downarrow,\uparrow$correspond to decimation and expansion, respectively.

4.1 Fast implementation case

In Figs. 1, 2, we display the analysis and synthesis procedures based on the first and second order interpolation. In the analysis, the signal $f_i(n)$ is sampled and then linearly fuzzified to get its membership function $\mu f_i\downarrow_{s}(n)$, fuzzy morphological interpolation give us $\mu\overline{f}_i(n)$ which is then linearly defuzzified to get its interpolated signal $\overline{f}_i(n)$. Decimation is then used to get the next level signal $f_{i+1}(n)$ which has the sampled points of the original signal, while $d_i(n)\downarrow$ has the error of the interpolated values. If we denote the linear fuzzifier (**L**), the membership interpolator (**H**) and linear defuzzifier (**D**) as Π_f (i.e., $\Pi_f\left(f_i\downarrow_{s}(n)\right)=\mathrm{D}\{\mathrm{H}[\mathrm{L}(f_i\downarrow_{s}(n))]\}=\overline{f}_i(n)$) then $f_{i+1}(n)=\Pi_f\left(f_i\downarrow_{s}(n)\right)\downarrow$ where $i=0,1,2,\cdots$. The $d_i(n)$ is the error signal of the interpolation i.e., $d_i(n)=f_i(n)-\Pi_f\left(f_i\downarrow_{s}(n)\right)$

In the synthesis, we proceed in an inverse fashion. The signal $f_{i+1}(n)$ is expanded and linearly fuzzified to get $\mu f_{i+1}\uparrow(n)$, then interpolated to get $\mu\overline{f}_{i+1}\uparrow(n)$, and finally linear defuzzified to get the interpolated signal $\Pi_f\left(f_{i+1}(n)\uparrow\right)=\overline{f}_i(n)$. The synthesis signal is $\hat{f}_i(n)=\Pi_f\left(f_{i+1}(n)\uparrow\right)+d_i(n)=f_i(n)$ indicating perfect reconstruction.

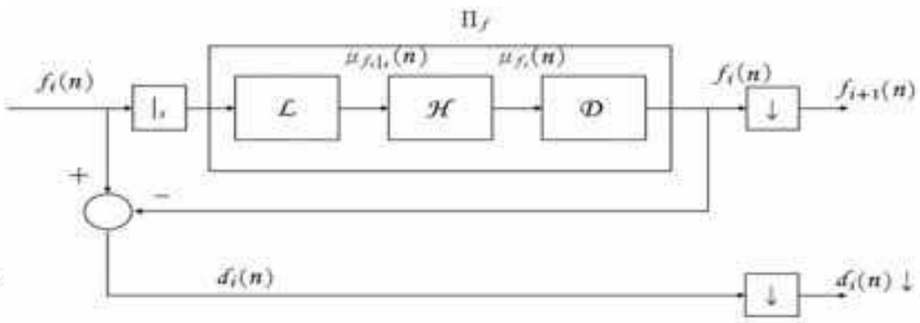

Fig.1. First and second order fuzzy morphological wavelet analysis

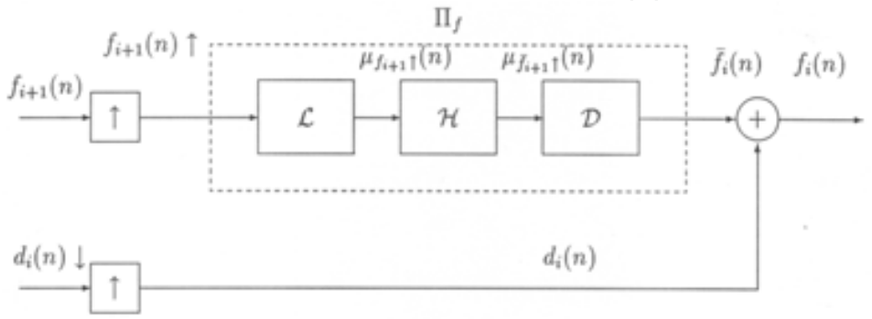

Fig. 2. First and second order fuzzy morphological wavelet synthesis

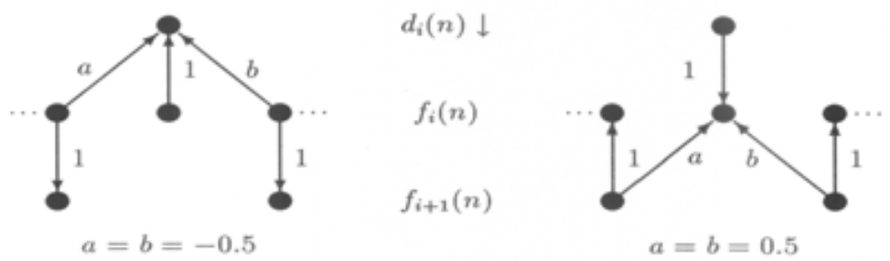

(a) (b)

Fig. 3. FMW pyramid implementation for first-order interpolator (a) analysis (b) synthesis.

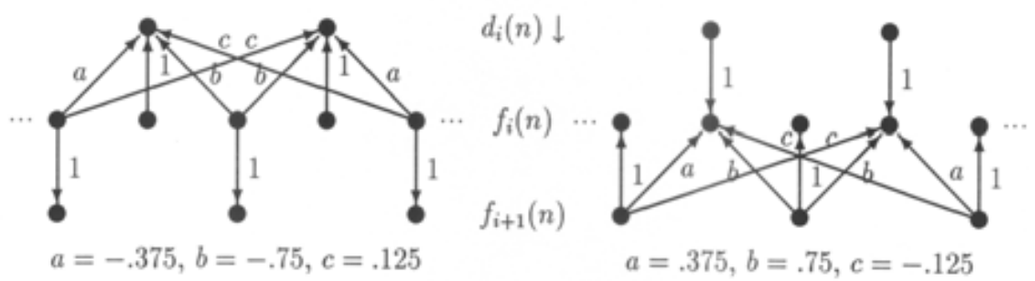

(a) (b)

Fig. 4. FMW pyramid implementation for second-order interpolator (a) analysis (b) synthesis.

A pyramid implementation for FMW representation using first order and second order interpolators in a window is shown in Figs. 3, 4, respectively. The FMW representation can be implemented very fast.

We further derive close formulas to get the smooth and detail signal of any level from the original signal when using first- and second-order interpolator. The usefulness of these properties will be clear when the representation is applied to the shape recognition.

Proposition 6. The pyramidal components of the FMW representation using a first-order interpolator has the following properties for $n = 0,1,\cdots; i = 0,1,\cdots$.

i. $f_i(n) = f_0(2^i n);$

ii. $d_i(n) = f_0(2^i(2n+1)) - \frac{f_0(2^{i+1}n) + f_0(2^{i+1}(n+1))}{2};$

Proposition 7. The pyramidal components of the FMW representation using a second-order interpolator has the following properties for $n = 0,1,\cdots; i = 0,1,\cdots$.

i. $f_i(n) = f_0(2^i n);$

ii. $d_i(2n) = f_0(2^i(4n+1)) - 0.375 f_0(2^{i+1}2n) - 0.75 f_0(2^{i+1}(2n+1)) + 0.125 f_0(2^{i+1}(2n+2));$

$d_i(2n+1) = f_0(2^i(4n+3)) + 0.125 f_0(2^{i+1}2n) - 0.75 f_0(2^{i+1}(2n+1)) - 0.375 f_0(2^{i+1}(2n+2));$

These propositions show that our smooth and detail signal of each level for the FMW representation can be obtained from the original signals and the number of pixels in the high level is smaller than that of the lower level. Notice that the first point of the smooth signal in every level is same as the first point in the original signal i.e. $f_i(0) = f_0(0), \forall i.$

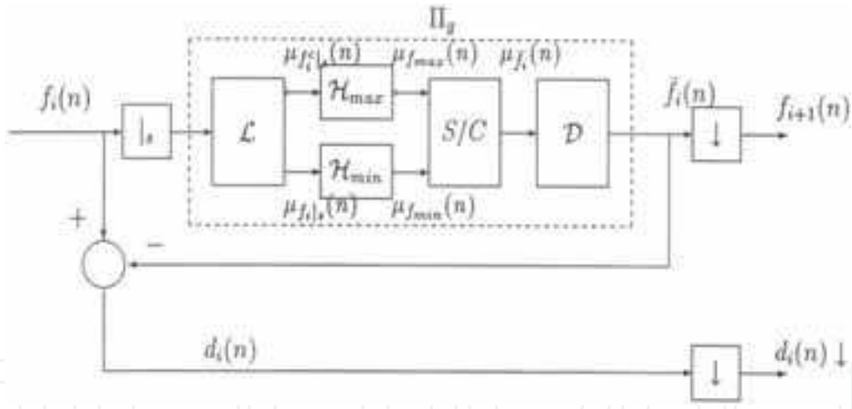

Fig. 5. Fuzzy morphological wavelet analysis (general)

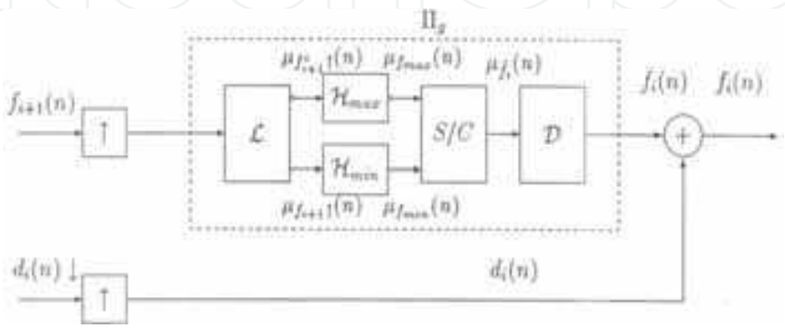

Fig. 6. Fuzzy morphological wavelet synthesis (general)

4.2 A general implementation case

When the order θ is three or more, the FMW analysis and synthesis blocks are shown in Fig. 5, 6, respectively. Perfect reconstruction is still possible as indicated before.

The interpolations are done using both minimum and maximum reconstruction, denoted as H_{max} and H_{min}, respectively. The block denoted as S/C is a selection and correction box, which is designed for choosing the maximum or minimum reconstruction as our interpolation output and correcting the error at sampled points. (see equation (20)-(23)).

5. Two-dimensional fuzzy morphological wavelet representation

The practical advantage of FMW becomes more evident in two-dimensions. The wavelet representation theory is much more complex in two-dimension than in one due to the difficulty of defining bivariate wavelets. Besides, the multirate methods in two-dimensions are more complex than in one-dimension to choose the sampling, decimation/expansion procedures. Although one-dimensional procedures can be applied when using separable two-dimensional filters, more appropriate non-separable filters make the procedure much more complex. The two-dimensional fuzzy morphological implementation is much simpler as it will be shown in the section.

5.1 Two-dimensional FMI

Unlike the one-dimensional case, there is no unique way to sample in two-dimension (Vaidyanathan, 1993). For simplicity, we consider two commonly used procedures: row/column sampling and quincunx sampling. Let $F=\{(m,n)\,|\,0\le m\le M-1,0\le n\le N-1\}$ be domain of the given signal $f(m,n)$ and $S=\{(m_1,m_2)\,|\,[m_1,m_2]^T=V[n_1,n_2]^T\}$ be the sampling domain, where V is a sampling matrix in lattice transform (Vaidyanathan, 1993) and $[\cdot]^T$ is transpose operator. For a given image $f(m,n),(m,n)\in F$ the sampling signal $f\downarrow_s(m,n)$ is defined as

$$f\downarrow_s(m,n)=\begin{cases} f(m,n) & (m,n)\in F\cap S \\ undefined & (m,n)\in F\cap \overline{S} \end{cases} \tag{24}$$

where the set $\overline{S}$ is a complement of set S. In lattice transform, the row sampling matrix (Vaidyanathan, 1993) is defined as

$$V_r=\begin{bmatrix} 1 & 0 \\ 0 & 2 \end{bmatrix} \tag{25}$$

So that for a given image $f(m,n)$, the row sampling $f\downarrow_s(m,n)$ yields

$$\begin{pmatrix} f(0,0) & * & f(0,2) & * & f(0,4) & \cdots & f(0,N-1) \\ f(1,0) & * & f(1,2) & * & f(1,4) & \cdots & f(1,N-1) \\ \vdots & \vdots & \vdots & \vdots & \vdots & \ddots & \vdots \\ f(M-1,0) & * & f(M-1,2) & * & f(M-1,4) & \cdots & f(M-1,N-1) \end{pmatrix}$$

where * corresponds to undefined samples. Similarly, for the column sampling matrix. The quincunx sampling matrix (Vaidyanathan, 1993) is defined as

$$V_q = \begin{bmatrix} 1 & -1 \\ 1 & 1 \end{bmatrix} \tag{26}$$

The quincunx sampling $f\downarrow_s(m,n)$ for the given image $f(m,n)$ is

$$\begin{pmatrix} f(0,0) & * & f(0,2) & * & f(0,4) & \cdots & f(0,N-1) \\ * & f(1,1) & * & f(1,3) & * & \cdots & * \\ f(0,0) & * & f(2,2) & * & f(2,4) & \cdots & f(0,N-1) \\ * & f(3,1) & * & f(3,3) & * & \cdots & * \\ \vdots & \vdots & \vdots & \vdots & \vdots & \ddots & \vdots \\ f(M-1,0) & * & f(M-1,2) & * & f(M-1,4) & \cdots & f(M-1,N-1) \end{pmatrix}$$

where * stands for undefined samples.

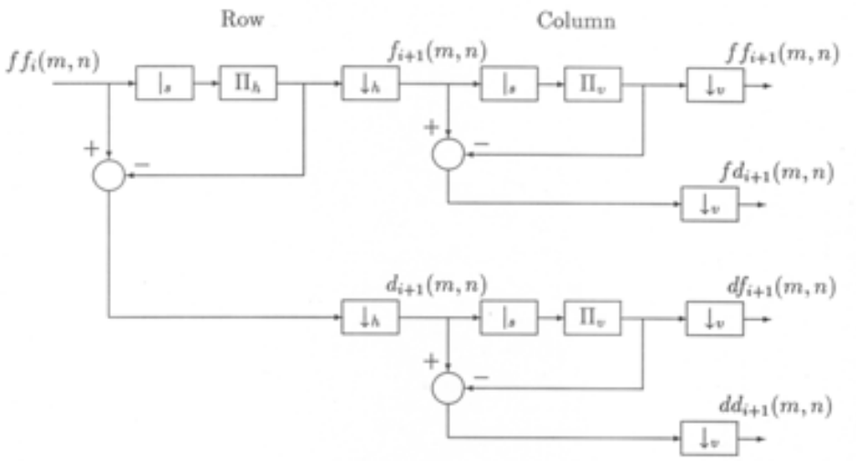

Fig. 7. FMW analysis block diagram for two-dimensional signals

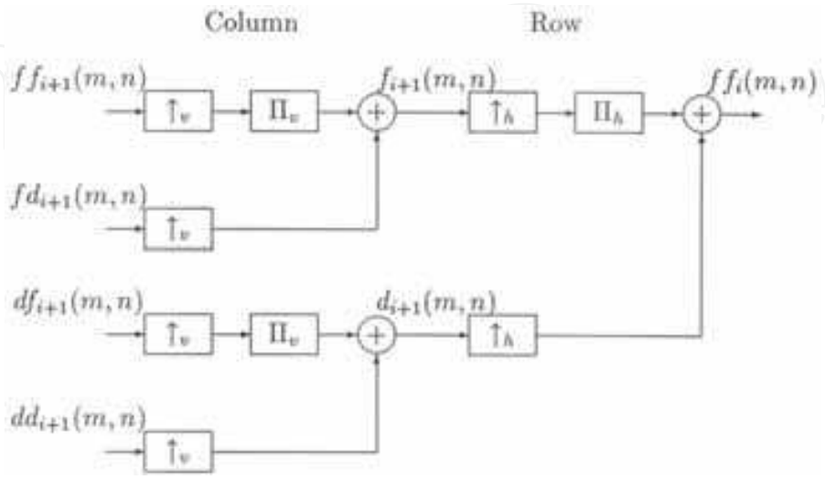

Fig. 8. FMW synthesis block diagram for two-dimensional signals

The interpolation in the row/column sampling can be done using the one-dimensional FMI discussed before. In the quincunx sampling case we extend the one-dimensional FMI algorithm using bivariate structuring functions. The structuring functions are generated as the product of one-dimensional ones. The structuring index ordering method in (Huang 1996) may be used to order these functions in two-dimensional space.

5.2 Two-dimensional FMW implementation

Figs. 7, 8 show the analysis and synthesis steps of the FMW representation using the row/column sampling. If the one-dimensional interpolator Π_x is first order we obtain the following relationship among the components for the analysis

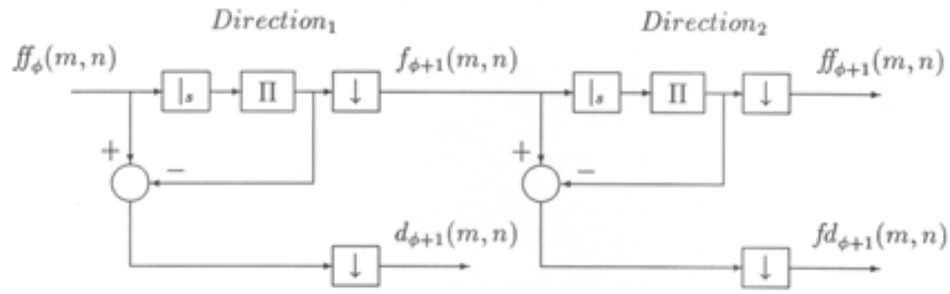

Fig. 9. TDFMW analysis block diagram with quincunx sampling

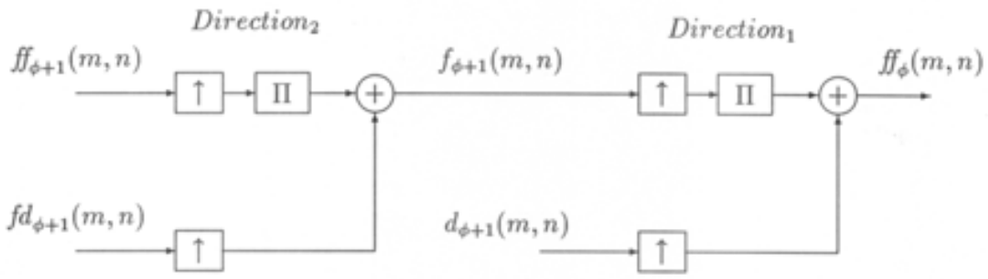

Fig. 10. TDFMW synthesis block diagram with quincunx sampling

1. $ff_{i+1}(m/2,n/2) = ff_i(m,n)$ m, n even
2. $fd_{i+1}((m-1)/2,n/2) = ff_i(m,n) - 0.5\left[ff_i(m-1,n) + ff_i(m+1,n)\right]$ m odd, n even
3. $df_{i+1}(m/2,(n-1)/2) = ff_i(m,n) - 0.5\left[ff_i(m,n-1) + ff_i(m,n+1)\right]$ m even, n odd
4. $$df_{i+1}((m-1)/2,(n-1)/2) = ff_i(m,n) - 0.5\left[ff_i(m,n-1) + ff_i(m,n+1) + ff_i(m-1,n) + ff_i(m+1,n)\right]$$ $$+0.25\left[ff_i(m-1,n-1) + ff_i(m-1,n+1) + ff_i(m+1,n-1) + ff_i(m+1,n+1)\right]$$

m, n odd and for the synthesis we get that

1. $ff_i(2m,2n) = ff_{i+1}(m,n)$
2. $ff_i(2m,2n+1) = fd_{i+1}(m,n) + 0.5\left[ff_{i+1}(m,n) + ff_i(m,n+1)\right]$
3. $ff_i(2m+1,2n) = df_{i+1}(m,n) + 0.5\left[ff_{i+1}(m,n) + ff_{i+1}(m+1,n)\right]$
4. $$ff_i(2m+1,2n+1) = dd_{i+1}(m,n) + 0.5\left[fd_{i+1}(m,n) + fd_{i+1}(m+1,n) + df_{i+1}(m,n) + df_{i+1}(m,n+1)\right]$$ $$+0.25\left[ff_{i+1}(m,n) + ff_{i+1}(m,n+1) + ff_{i+1}(m+1,n) + ff_{i+1}(m+1,n+1)\right]$$

Notice that if we use column/row instead of row/column sampling the signals $ff_{i+1}(m,n)$ and $dd_{i+1}(m,n)$ remain the same while $fd_{i+1}(m,n)$ and $df_{i+1}(m,n)$ are interchanged.

When the quincunx sampling is used, the Π is a TDFMI. The image is processed block by block. The structures of the analysis and synthesis are shown in Fig. 9, 10, respectively.

		Piles			Pepper		
stage		1	2	3	1	2	3
FMW	r/c	0.689	0.552	0.503	0.703	0.562	0.512
	q	0.697	0.565	0.519	0.708	0.584	0.531
WT	r/c	0.642	0.501	0.469	0.658	0.509	0.476

Table 1. Compression ratio for two-dimensional signal

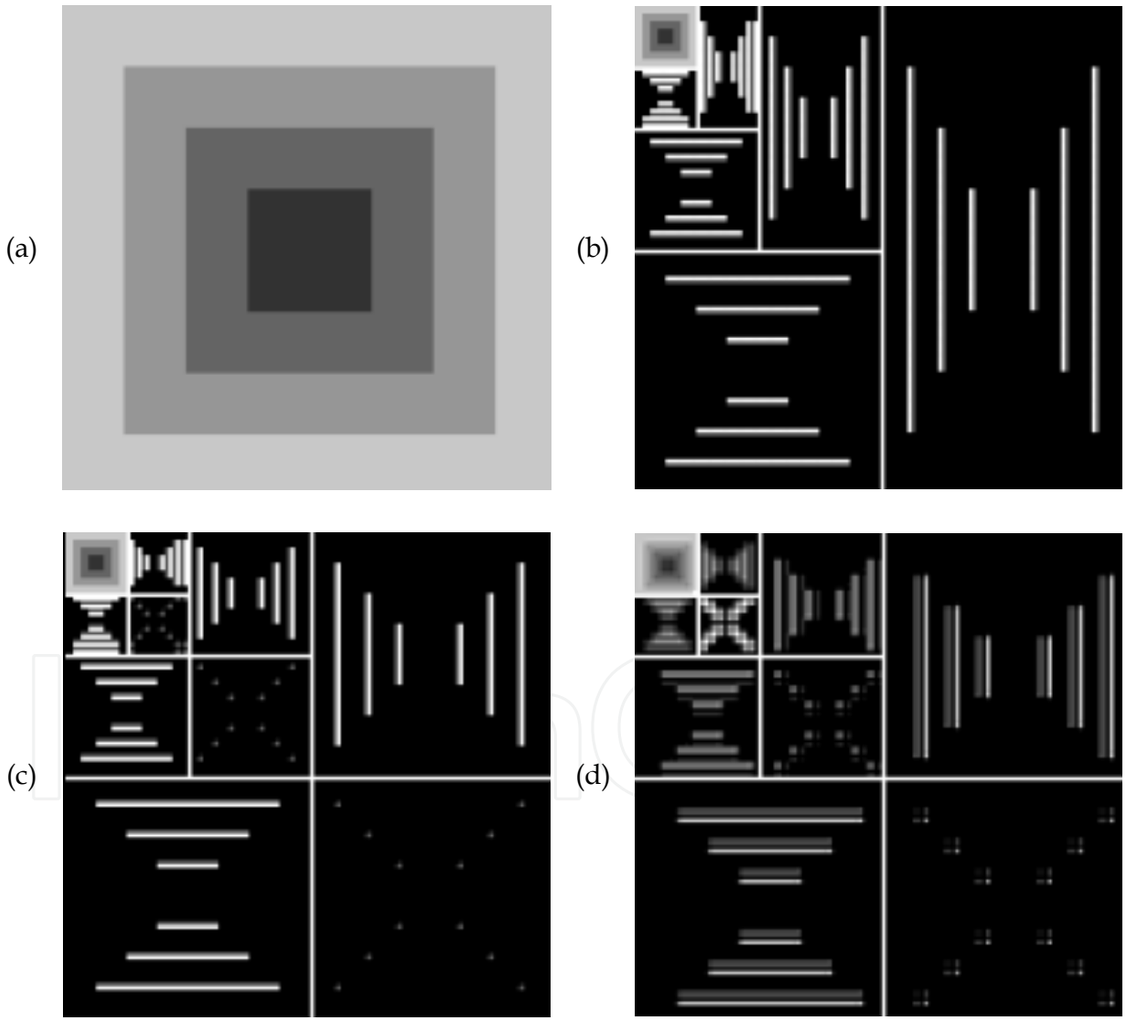

Fig. 11. Two-dimensional FMW and WT representation for artificial image: (a) original image, (b) TDFMW using quincunx sampling, (c) TDFMW using row/column sampling, (d) WT using row/column sampling.

6. Applications

To illustrate our representation, we show how it can be applied to data compression and shape recognition. We compare the data compression results with those using Daubechies' wavelet transform (Daubechies, 1988) and the shape recognition results with Fourier descriptor method (Gonzales & Woods, 2002, Persoon & Fu, 1977).

6.1 Data compression

The application of FMW representation for data compression is achieved by encoding the lowest resolution smoothed image and the detailed image. The performance of our representation is evaluated by the entropy-based compression ratio (ECR) defined as

$$\mathrm{ECR} = \frac{\sum_{i=0}^{N-1} M_i \ell_i}{M_T \ell_T} \tag{27}$$

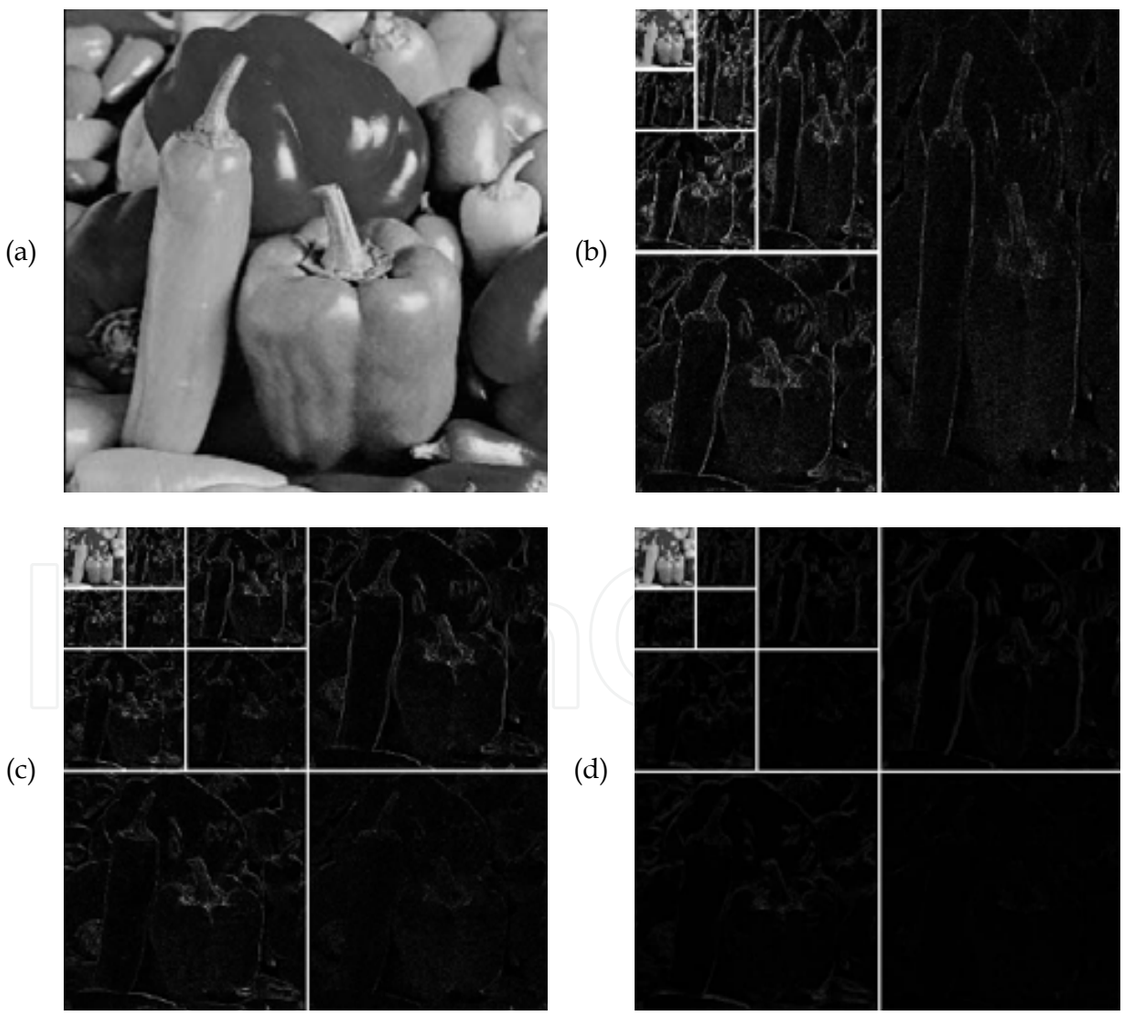

Fig. 12 Two-dimensional FMW and WT representation for pepper image

where N is the number of subblock signals, M_i is the number of samples of the subblock i, ℓ_i is the bits/sample required to code subblock i, ℓ_T is the bits/sample required for the original signal, M_T is the total number of samples of the original signal. The average bits/sample ℓ_i required to code a subblock signal is defined by entropy as:

$$\ell_i = -\sum_{j=0}^{G-1} p_j \log_2 p_j \tag{28}$$

where p_j is a probability of a sample with amplitude j, G is the greatest amplitude of the signal.

The TDFMW representation is used to process the artificial (piles) and real (pepper) images. The TDFMW pyramid representations for piles image in Fig. 11 (a) are shown in Fig. 11 (b) and (c) using quincunx and row/column sampling with frame size of 3×3, respectively. For comparison, the result of WT using Daubechies' wavelet of length 8 is shown in Fig. 11 (d) using row/column sampling. The TDFMW pyramid representation for pepper image in Fig. 12 (a) are shown in Fig. 12 (b) and (c) using qucunx and row/column sampling with window size of 3×3, respectively. For comparison, the WT using Daubechies' wavelet of length 8 and row/column sampling method is shown in Fig. 12 (d). The data compression results for FMW and WT are shown in Table 1 for three stages.

(a) (b)

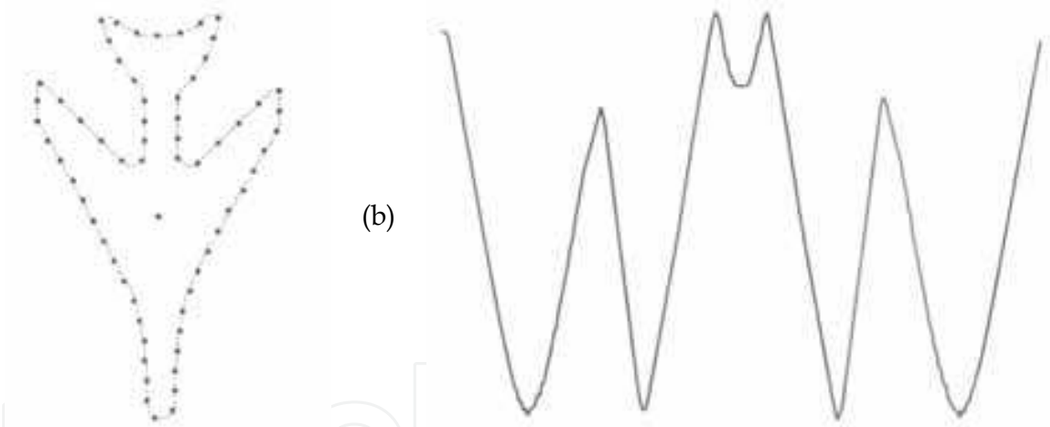

Fig. 13. Signature extraction: (a) shape sampling (b) signature

6.2 Aircraft shape recognition

In this section, we apply our FMW representation to aircraft shape recognition. The shapes are nonoverlapping, simply connected and closed planar contours, each represented by a set of boundary coordinates $\{(x(n),y(n)),n=0,1,2,\cdots,N-1\}$. Due to closeness of the contour, the resulting observations are periodic i.e., $x(n)=x(n+N)$ and $y(n)=y(n+N)$. We compute the centroid, sample the boundary at equidistant points to calculate corresponding radii $\{r(n),n=0,1,2,\cdots,M-1\}$ where M is usually less than N (Fig. 13(a)). These radii $\{r(n),n\in[0,M-1]\}$ form a one-dimensional signature (Fig. 13(b)) of the two-dimensional contour, which is invariant to translation, but it does depend on rotation and scaling [26].

In order to use the signature signal for shape recognition we need to overcome this dependence. When applying the FMW representations of the template and the test shapes, the linear fuzzification obviates the scaling dependence. The rotation of the object generates a signature that is shifted in a periodic way with respect to the template signature. To find a reference point we will then apply proposition 6 or 7 to do so. Basically these propositions establish that $\{f_0(0) = f_i(0), \forall i\}$, that is that at every stage in the FMW the first point is the same for every stage in the representation. By working from the lowest to highest resolution of the FMW representation, we then try to match the template signature with the test signature. The matchness is determined by the nearest-neighbor rule (Schalkoff, 1992) using the Euclidean distance between template and test signatures. This can be done by initiating the lowest resolution template signature with a known maximum and then sequentially shifting the lowest resolution test signature until either a match or a mismatch situation is encountered. If a match is obtained then we verify that it is a good match and stop, or consider the next higher resolution and repeat this process. The verification uses the detail signals of the FMW of the template and test signature.

60 test shapes used in the experiment are obtained by scaling, rotating the template shapes in Fig. 14, 10 scales from 1.0 with 0.15 increase in each step and 10 rotations from 0 with 15 degree increase in each step and then sample them to get the test signatures. As an example of the resulting test shapes is shown in Fig. 15. The shapes are all discriminated at the 6^{th} level which contains 4 pixels. These results verify that using our FMW representation can effectively solve the scaling and rotation variant problem.

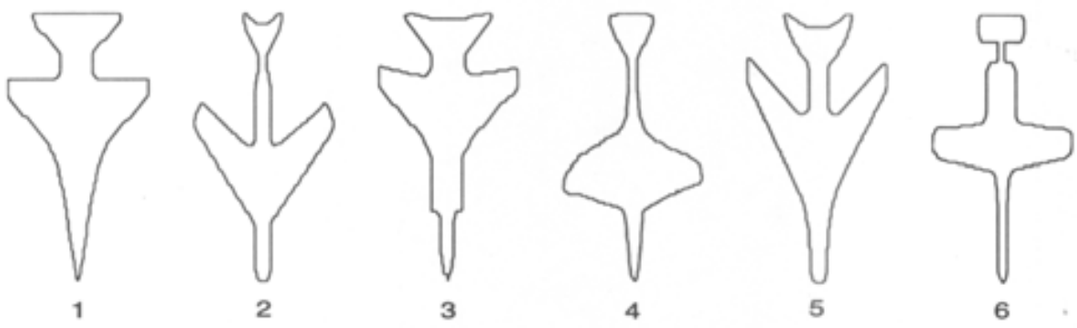

Fig. 14. Template aircraft shapes

For comparison purpose, the Fourier descriptor is used to do the same experiment. The nearest-neighbor rule is used to classify the shapes by Euclidean distance between the Fourier coefficients of the template and test shape. The results are that only the shapes without scaling and rotation is correctly classified surely when coefficients is greater than 4. The correctly classified shapes when using 16 coefficients are only 17 out of 60 (28 percent). The discrimination performance can be improved to recognize around 90 percent by the Fourier descriptor using optimal matching algorithm, however, the computation complexity will increase up to 94 times as described in (Persoon & Fu, 1977). These results show that our recognition method has better performance over the Fourier descriptor in recognizing the aircraft shapes.

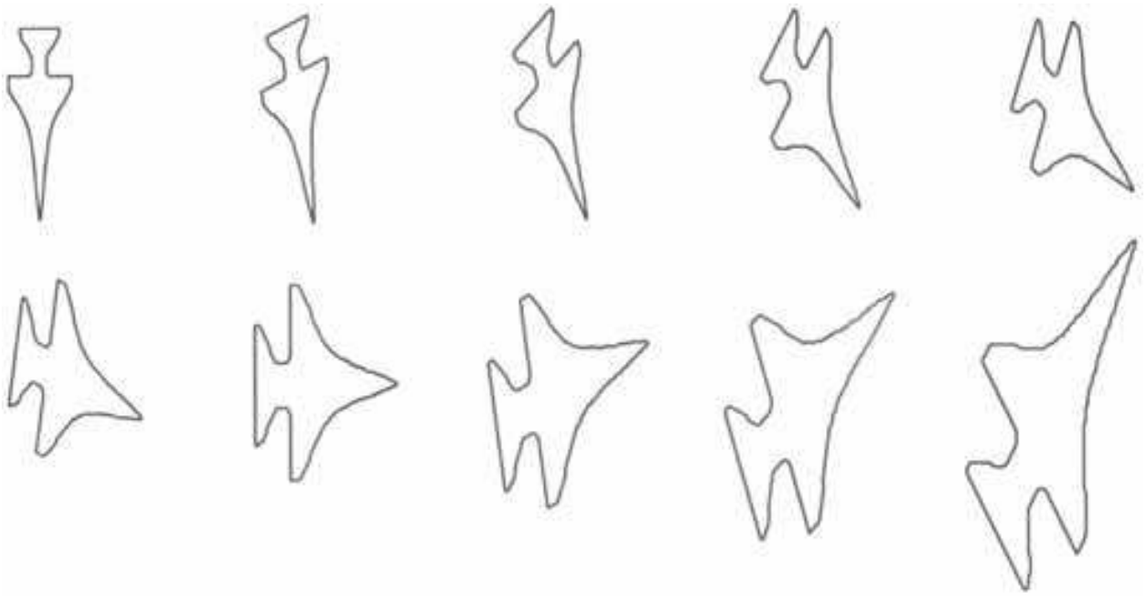

Fig. 15. Test aircraft shapes example

7. Conclusion

A novel image representation using fuzzy morphological approach has been presented in this paper. Using the fuzzy morphological operators and the minimum and maximum reconstruction we develop the fuzzy morphological interpolation (FMI) algorithm. Based on FMI and the hierarchical pyramid structure, we formulate the analysis and synthesis procedure, similar to those given by wavelet transform. Through using the fuzzy morphological approach, a signal can be efficiently represented with several additional advantages, such as lower computation complexity and easily extend to two dimensions. Furthermore, our representation can be implemented very fast by parallel. We successfully use the fuzzy mathematical morphology approach to extend the work of the Pitas and Venetsanopoulos and of Song and Delp on morphological signal representation. We have applied our representation to image analysis and shape recognition, the experimental results have shown the advantage of using our FMW representation as compare with the WT (Daubechies, 1988) and Fourier descriptor (Persoon & Fu, 1977) methods.

8. References

Bandemer, H. & Nather, W. (1992) *Fuzzy Data Analysis*. Kluwer Academic Publishers.

Burt, P. J. & Adelson, E. (1983) Laplacian pyramid as a compact image code, *IEEE Trans. on Communication*, Vol. COM-31, pp. 532-540.

Cha, H. & Chaparro, L. F. (1998) Adaptive morphological representation of signals: polynomial and wavelet methods, *Multidimensional Systems and Signal Processing*.

Daubechies, I. (1988) Orthonormal bases of compactly supported wavelets, *Comm. on Pure and Applied Math.*, vol. 41, pp. 909-996.

Dubois, D. & Prade, H. (1980)*Fuzzy Sets and systems theory and applications*. Academic Press.

Gonzales, R. & Woods, R. E. *Digital image processing*. Prentice-Hall, 2002.

Goutsias, J. & Heijmans, H. J. A. M. (2000) Nonlinear multiresolution signal decomposition schemes—PartI: Morphological pyramids, *IEEE Trans. on Image Processing*, vol. 9, pp. 1862-1876.

Haralick, R. M. Sternberg, S. R. & Zhuang, X. (1987) Image analysis using mathematical morphology, *IEEE Trans. on Pattern Analysis and Machine Intelligence.*, vol. PAMI-9, no. 4, pp. 532-550,.

Haralick, R. M. Zhuang, X. Lin, C. & Lee, J. (1989) The digital morphological sampling theorem, *IEEE Trans. Acoustics, Speech, and Signal Processing*, vol. 37, no. 12, pp. 2067-2090, 1989.

Heijmans, H. J. & Toet, A. (1991) Morphological sampling, *CVGIP-Image understanding*, vol. 54, no. 3, pp. 384-400.

Heijmans, H. J. A. M. & Goutsias, J. (2000) Nonlinear multiresolution signal decomposition schemes—PartII: morphological wavelet, *IEEE Trans. on Image Processing*, Vol. 9, 1897-1913.

Huang, C. P & Chaparro, L. F. (1995) Signal representation using fuzzy morphology, *Proc. ISUMA-NAFIPS (IEEE Computer Press 1995)*, pp. 607-612.

Huang, C. P. (1996) *Signal representation using fuzzy morphology and its applications*, Ph.D. Dissertation, University of Pittsburgh, Pittsburgh , PA.

Kronander, T. (1987) Sampling of bandpass pyramid, *IEEE Trans. on Communication.*, vol. COM-35, no. 1, pp. 125-127.

Mallat, S. G.(1989) Multifrequency channel decompositions of images and wavelet models, *IEEE Trans. Acoustics, Speech, and Signal Processing*, vol. 17(12) , pp. 2091-2110.

Neuman, C. P. & Schonbach, D. I. (1974) Discrete (legendre) orthogonal polynomials —a survey, International Journal for Numerical Methods in Engineering, vol. 8, pp. 743-770.

Persoon, E. and Fu, K. S. (1977) Shape discrimination using fourier descriptors, *IEEE Trans. on Systems, Man, and Cybernatics*, vol. SMC-7, no. 3, pp. 170-179.

Pitas, I. & Venetsanopoulos, A. N. (1990) Morphological shape decomposition, *IEEE Trans. Pattern Analysis Machine Intell.*, vol. 12, pp. 38-45,

Pitas, I. & Venetsanopoulos, A. N. (1991) Morphological shape representation, in *Proc. IEEE Inter. Conf. on ASSP*, (Toronto, Canada), pp. 2381-2384.

Pitas, I. (1990) Morphological signal decomposition, in *Proc. IEEE Inter. Conf. on ASSP*, (New Mexico), pp. 2169-2172.

Schalkoff, R. (1992) *Pattern Recognition Statistical, Structural and Neural Approaches*. John Wiley and Sons.

Serra, J. (1982) *Image Analysis and Mathematical Morphology*. New York: Academic.

Sinha, D. & Dougherty, E. R. (1992) Fuzzy mathematical morphology, *Journel of Visual Communication and Image Processing*, pp. 286-302.

Song, J. & Delp, E. J. (1990) The analysis of morphological filters with multiple structuring elements," *Computer Vision, Graphics, and Image Processing*, vol. 50, pp. 308--328.

Sternberg, S. R. (1983) Biomedical image processing, *IEEE Computer Mag.*, vol. 16, pp. 22-34.

Vaidyanathan, P. (1993) *Multirate Systems and Filter Banks*, Prentice Hall.

Zadeh, L. A. & Fu, K. S. & et al., ed. (1975) *Fuzzy Sets and Their Applications to Cognitive and Decision Processes*. Academic Press,Inc..

Zadeh, L. A. (1965) Fuzzy sets, *Information and Control*, vol. 8, pp. 338--353.

Pattern Recognition Techniques, Technology and Applications

Edited by Peng-Yeng Yin

ISBN 978-953-7619-24-4
Hard cover, 626 pages
Publisher InTech
Published online 01, November, 2008
Published in print edition November, 2008

A wealth of advanced pattern recognition algorithms are emerging from the interdiscipline between technologies of effective visual features and the human-brain cognition process. Effective visual features are made possible through the rapid developments in appropriate sensor equipments, novel filter designs, and viable information processing architectures. While the understanding of human-brain cognition process broadens the way in which the computer can perform pattern recognition tasks. The present book is intended to collect representative researches around the globe focusing on low-level vision, filter design, features and image descriptors, data mining and analysis, and biologically inspired algorithms. The 27 chapters coved in this book disclose recent advances and new ideas in promoting the techniques, technology and applications of pattern recognition.

INTECH
open science | open minds

InTech Europe
University Campus STeP Ri
Slavka Krautzeka 83/A
51000 Rijeka, Croatia
Phone: +385 (51) 770 447
Fax: +385 (51) 686 166
www.intechopen.com

InTech China
Unit 405, Office Block, Hotel Equatorial Shanghai
No.65, Yan An Road (West), Shanghai, 200040, China
中国上海市延安西路65号上海国际贵都大饭店办公楼405单元
Phone: +86-21-62489820
Fax: +86-21-62489821

IntechOpen